Aerial Interaction Control Using Gain-Scheduling and PID for a Drone with a 2-DOF Arm

Aaron Lopez Luna*, Jose Martinez Carranza, and Israel Cruz Vega
National Institute of Astrophysics, Optics and Electronics

ABSTRACT

One of the significant challenges of unmanned aerial vehicles (UAV) is the physical interaction with an object or a rigid structure. There are numerous potential benefits of physical interaction with the environment. However, the process of approaching a UAV to an object or a surface also brings challenging control problems. This paper addresses the control problem of a UAV endowed with a robotic arm to physically contact a rigid structure. The proposed control technique is based on a Gain-Scheduled Proportional-Integral-Derivative (GS-PID) algorithm. Our previous work [1] based on a simple Gain-Scheduling (GS) approach for the stability of the robotic aerial system is insufficient to counteract the disturbances during the interaction successfully. Therefore, the proposed GS-PID control can respond to the disturbances induced by the wall-effect, the arm's movement, and the contact with the rigid structure. Experimental testing results demonstrate satisfactory performance of the proposed control strategy.

1 INTRODUCTION

Aerial manipulators (robotic manipulator arms attached to aerial vehicles) research has grown in recent years due to the importance and potential applications of this useful systems in industrial and commercial fields. [2, 3]. Nevertheless, this new configuration represents a new problem in the stability control of the aerial vehicle. The movements of a manipulator attached to a UAV during flight mode are considered as disturbances, which can cause instability and the loss of the entire system. New models and control algorithms have been proposed to prevent this situation [4, 5]. The UAV physical interaction may provide excellent solutions as well as reliable operations, e.g., the inspection of a surrounding environment. Moreover, the concept called flying hand is a unique and leading technology. However, the interaction control imposes inherent nonlinearities due to not only the dynamic behavior of the UAV but also the interaction between the surface and the system [6, 7]. In all the situations in which contacts between the aerial vehicle and the environment occur, the dynamics of the system may dramatically change, and the development of a robust control law able to handle all the possible interactions becomes a challenge [7, 8].

In this work, we consider the proposal of taking into account dynamical changes in the UAV due to three essential factors. i)The movement of the arm attached to the aerial vehicle, ii) the wall-effect disturbance when the system is approaching the rigid structure, and iii) the effect of the contact with the surface. We also propose an experimental study to determine the variation in plant dynamics with the three factors and establish a set of controllers which allows approximating the real trajectory of the system to the desired trajectory. Therefore in this work, we employ a novel manipulator arm of two degrees of freedom (DOF) especially developed for a commercial quadcopter parrot bebop-2. We also propose to incorporate a GS approach to the Classical PID control to ensure the stability of the proposed aerial manipulator. We determine the gain values of a set of PID controllers by the experimental study; this represents a novel technique to deal with the drawbacks of perturbations in the aerial manipulation systems.

This paper is organized as follow: In section 2, the proposed system is described. The GS-PID control technique developed for this work is presented in section 3.1. To prove the effectiveness of the proposed strategy, a set of experiments are implemented and are described in section 4; the experimental results are also shown in this section. Finally, the main contribution, conclusions, and future direction are described in section 6.

2 DESCRIPTION OF PROPOSED SYSTEM

Nowadays exist different configurations of UAV systems used for several missions in commercial and industrial tasks. Each configuration has distinct advantages and disadvantages according to its design. Vertical Take-Off and Landing (VTOL) vehicles have been taken into account especially for aerial manipulation due to specific aspects of their flight mode which are used to achieve the primary goal of maintaining a manipulator robot in the desired point. In this work, we designed an aerial, consisting of two main subsystems: The aerial vehicle of four rotors and a robotic arm of two DOF. In the following subsections, each one of this system is presented.

*Email address(es): aaron.eleazar@inaoep.mx

2.1 ROBOTIC ARM

For manipulation and interaction task, robotic arms can provide the necessary degrees of freedom to achieve the objective [9, 10]. In contact with the environment, for example, an n-DOF arm could supply the stiffness and versatility to the vehicle to accomplish the goal involving contact with a rigid structure. The n-DOF arm could also provide a safe distance between the aerial system and the structure.

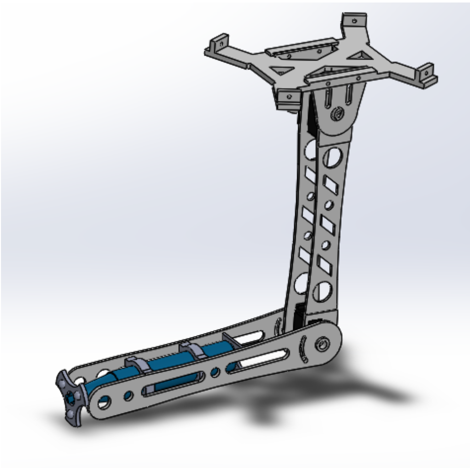

Figure 1: CAD model of proposed robotic arm.

The robotic arm of Fig. (1) was developed thinking in two main aspects - first, the physical task. The task consists in to exert a force on a rigid surface. For this objective, the robotic arm must provide the movements necessaries to contact the surface successfully and also must provide adequate distance between the vehicle and the surface to reduce the disturbances induced by the proximity of the rigid structure with the rotors of the aerial vehicle. Second, the dimensions of the proposed design must maintain a relationship with the physical capabilities of the system in order to guarantee the ideal performance in flight mode. Even with this consideration, the behavior of the robotic arm can alter the efficiency of the vehicle, for this reason, a control technique considering the perturbations of the robotic arm must be implemented to achieve the proposed task. The length of the extended arm designed for this work provides sufficient distance between surface and the aerial system to maintain a safety flight and reduce the wall effect disturbance. the arm structure is light enough to allow the aerial system to take off suitably and keep a stable flight, however, the poor stiffness of the arm it must be considered in the control design to prevent exceed supported force of the arm. In the following sections, the problem of perturbations and the proposed solution is handled.

2.2 END EFFECTOR

To prove the satisfactory performance of the interaction control, we proposed an experimental scenario in which the aerial manipulator marks the points where the end-effector of the arm and the surface are in contact. A set of pieces were designed, allowing the arm to hold a pencil and mitigate the friction and contact forces. Fig. (2) shows the proposed end-effector for the experimental task. The design of the contact end-effector permit to reduce the interaction area to a three simple points, reducing at the same time the friction in the contact phase.

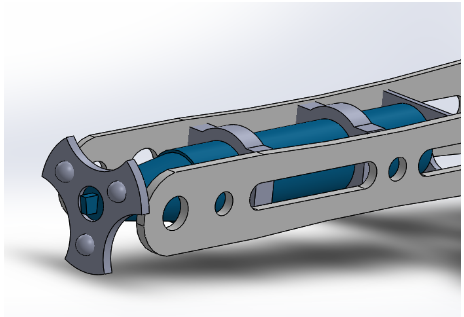

Figure 2: CAD model of end effector for contact whit a surface.

2.3 PHYSICAL SYSTEM

Due to the four rotors, the quadcopter has more lifting power than a helicopter of the same size, allowing carry a more massive payload. The interest in this kind of configuration comes not only from its dynamics, which represent an attractive control problem but also from the design issue [11, 12, 13, 14]. The rotors of a quadcopter work together to lift the weight of the quadcopter airborne. Quadcopters have being used in search and rescue missions, surveillance, inspection, mapping, and law enforcement [15]. Fig. (3) shows the complete physical system, the bebop-2 with the 2-DOF arm.

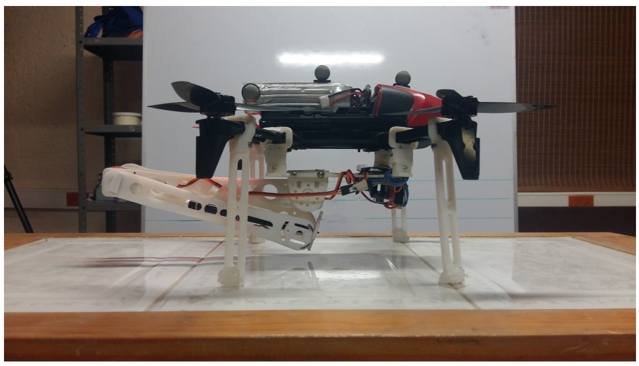

Figure 3: Aerial manipulator, physical implementation.

3 AERIAL INTERACTION CONTROL

In this work, the PID control and the Gain-Scheduling approach are developed to design and implement an interaction control for a bebop-2 vehicle with a 2-DOF arm. The following section describes the architecture of the controls and the system structure.

3.1 PID CONTROL

A PID controller continuously calculates an error value $e(t)$ as the difference between the desired set point and the measured process variable and applies a correction based on proportional, integral, and derivative terms, (sometimes denoted P, I, and D respectively). The following equation (1) describes the PID algorithm:

$$u(t) = k_p e(t) + k_I \int e(\tau) d\tau + k_D \frac{d}{dt} e(t) \quad (1)$$

where k_p, k_I, k_D are the PID control gains, $u(t)$ is the control signal and $e(t)$ is the error signal. The integral, proportional, and derivative parts are interpreted as control actions based on the dynamics of the signal. The PID gains can be designed based upon the system parameters with a certain precision. In this work, a PID controller is designed for the x and y position and yaw orientation of the aerial vehicle.

3.2 GAIN SCHEDULING CONTROLLER

To compensate the disturbances of the robotic arm, we incorporate the Gain-Scheduling technique into the PID control, enhancing the performance of the flight vehicle with a robotic arm. The gain-scheduling method uses measurable variables correlating changes in the dynamic process to define controller parameters. The gain schedule technique is an acceptable approach to control nonlinear systems using a set of linear controllers, providing adequate control responses to various operational points of the system. To tune the controller, we need to select one or more adjustment variables.

After the selection of these variables, the regulator parameters are calculated for several operation points. In this work, for the designing of the GS-PID controller, a set of pre-tuned gains are applied to the controllers. No rule specifies the number of zones or operation points for the division in the range of operation of the plant, the designer decides in this respect [16, 17, 18]. To implement the GS-PID controller, we follow the next steps: first, to chose auxiliary variables. In this work, these variables are the angles of the links of the robotic arm (θ_1, θ_2). Second, after choosing the auxiliary variables, the operation points P_n are determined. These operation points are the position P_e in (X, Y, Z) of the end effector of the arm which depends on the values of θ_1 and θ_2 (More detail in [1]). The controller actions readjusted for each operating condition. The calculated parameters are the gains K_p, K_I, and K_D of the PID control, which now depends on the values of θ_1 and θ_2. The equation (1) with the gain-scheduling method now is rewritten as follow:

$$u = k_p(\theta_{1,2})e + k_I(\theta_{1,2}) \int e(\tau)d(\tau) + k_D(\theta_{1,2}) \frac{d}{dt} e(t) \quad (2)$$

where $k_P(\theta_{1,2})$, $k_I(\theta_{1,2})$, $k_D(\theta_{1,2})$ are the PID control gains for every operational condition P_n. The following section describes the implementation of GS-PID controller for the aerial vehicle.

3.3 WALL-EFFECT AND CONTACT DISTURBANCE

When a UAV in flight mode is close to a wall (vertical rigid structure) a disturbance force induced by the propellers of the aerial vehicle affects the stability of the system, this disturbance increase when the distance between the vehicle and the surface is smaller. Due to the length of the arm, it is not sufficient to maintain the aerial vehicle far enough to decrease the wall-effect, so such disturbance must be considered to achieve the interaction task satisfactorily. The contact with the surface also generate a rejection force affecting the flight stability; this rejection force depends on the contact force exerted by the arm. To simplify the interaction control, the contact force of the arm is considered to stay at a minimum value. We conducted experiments to obtain both the wall-effect and the contact rejection force.

4 EXPERIMENTAL SETUP

The proposed control strategy was proved via experimental tests in a controlled environment. The manipulator incorporated to bebop-2 is composed of 2 links with a dimension of 10 cm (L), 0.3 cm (W) and 4 cm (H), each one with 0.12 kg (m). In order to compensate the disturbance of the arm with the GS-PID controller for the position (X, Y, Z) of the system, a set of ten operation points were chosen carefully for each controller. Fig. (4) shows the operation points of the system depending on the angles of the links.

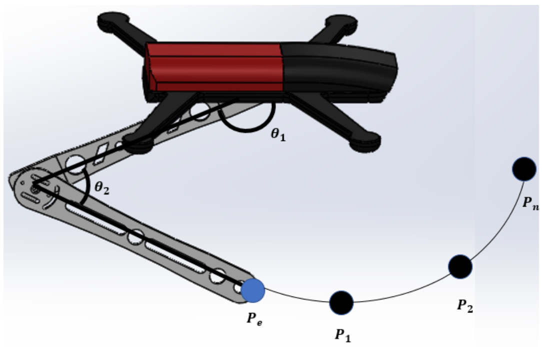

Figure 4: Representation of operating points of the system [1].

Just like in the previous work [1] the VICON cameras were used to get the actual position (X, Y, Z) of the system continually and monitoring the variables θ_1 and θ_2 of the links of the robotic arm.

Fig. (5) depicts the block diagram for this research. In this representation $E(t)$ is the error between the desired position and the actual position, $Y(t)$ represents the control signals sent to the aerial vehicle to control the (x, y, z) position. The real position of the aerial vehicle during flight mode is taken from the VICON system providing information used to calculate $E(t)$. The different positions of the robotic arm produce different disturbances which can be calculated using the error as a reference to the displacement of the system; this instability is represented as noise in the block diagram affecting the position of the vehicle directly. The objective is to compensate for this displacement to maintain the aerial vehicle in the desired position.

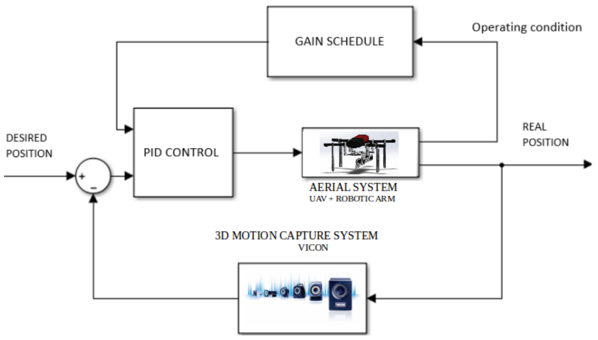

Figure 5: Block diagram of the proposed system with GS-PID control [1].

A set of gains were obtained experimentally to compensate the disturbances and upgrade the performance of the control maintaining the system in the desired position. Table 1 shows the value of K_p, K_I and K_D for each operating point.

θ_1/θ_2	K_P	K_I	K_D
0/0	0.22	0.12	0.03
30/0	0.45	0.37	0.09
30/30	0.92	0.64	0.17
60/30	1.3	0.9	0.22
90/30	1.6	1.2	0.56
120/30	1.72	1.34	0.78
150/30	2.1	1.66	1.05
150/90	2.22	1.79	1.12
150/120	2.45	1.89	1.2
150/150	2.52	1.98	2.31
near to wall	4.56	2.02	2.62

Table 1: set of gains for the operating points

Additionally, to the gains obtained in the previous work [1], a set of experiments were made to calculate the wall-effect affecting the stability of the system. Fig. (6) shows the experiment where the system is near to a vertical surface.

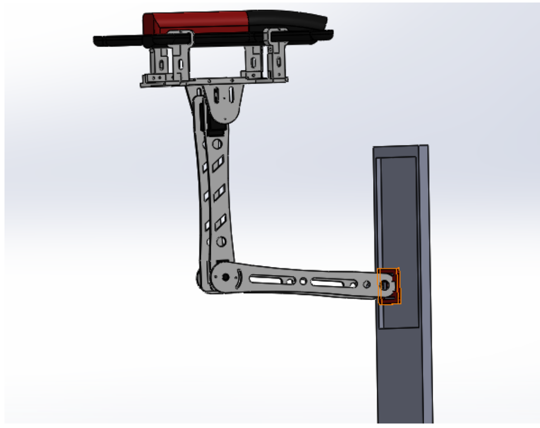

Figure 6: Representation of desired interaction task.

5 RESULTS

This section contains the experimental results of the proposed system. Three different experiments were designed, to demonstrate the effectiveness of the GS-PID interaction control. First, analyzing the behavior of the system when it is trying to approximate the surface employing a standard PID control. The x-axis of the graph represents time in milliseconds (ms), and the y-axis of the graph represents the position in millimeters (mm). The desired position of the system is (15,0, 1), at 20 cm near the surface. Fig. (7) shows the response of the system. The system is unable to reach the references in the x-axis due to the wall-effect.

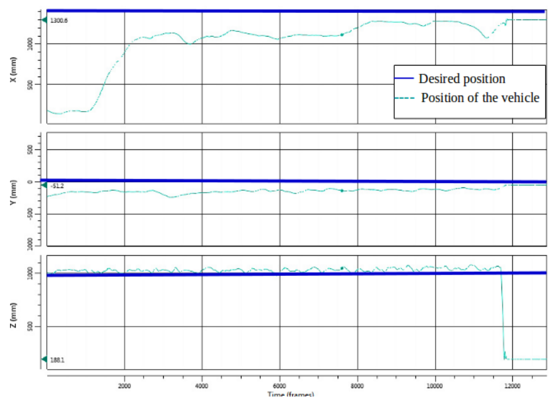

Figure 7: Behavior of the aerial vehicle carrying the robotic arm with standard PID control.

In the second experiment, GS-PID control is implemented [1]. This time, the control includes the set of gains required to attenuate the wall-effect, Fig. (8) shows the behavior of the system, the GS-PID control can lead the system to the reference.

In the third experiment, the end-effector is now in contact with the rigid surface, and the system executes a horizontal movement to follow a linear trajectory in the surface. The

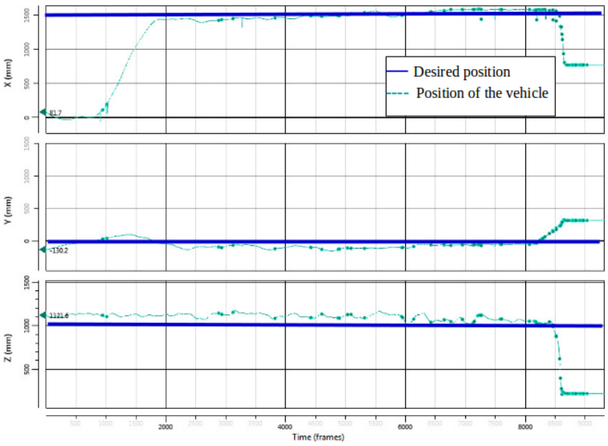

Figure 8: Behavior of the aerial vehicle with the robotic arm extended near to rigid surface, GS-PID control

GS-PID control maintains the system at the required distance to the surface to achieve the task. Fig. (9) shows the successful contact of the system with the surface.

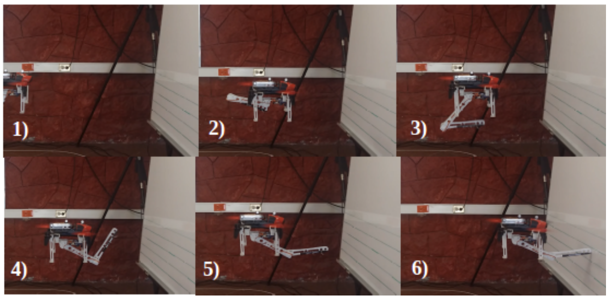

Figure 9: Sequence of successful contact of the aerial manipulator with the rigid surface.

Fig. (10) shows the response of the system in full contact with the surface. The proposed control maintains a constant distance between the system and the surface while the manipulator moves in the y-axis, drawing the continuous line over the surface.

The final result proves the effectiveness of the proposed control to interact with the environment. For quantitatively compare the control performance, we defined the following function:

$$mse = \frac{1}{n}\sum_{i=1}^{n}(p_d - p_r)^2 \tag{3}$$

this equation describes the mean squared error (mse) between p_d, as the desired position, and p_r the real position of the system in the step time i. The quantitative results for each controller are given in Table 2. We can observe an upgrade in the performance and response in comparison with the classical PID control.

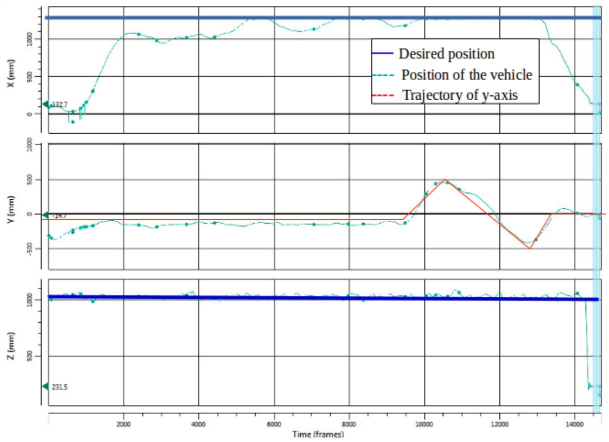

Figure 10: Behavior of the aerial manipulator in full contact with the rigid surface, GS-PID control.

mse	PID control	GS-PID control.
X	42.56	2.12
Y	26.44	1.23
Z	7.65	0.17

Table 2: Mean squared error.

In Figure 11 a line drawn by the drone is shown. The line proves the effectiveness of the proposed control to maintain the system in constant contact with the structure. We aim to upgrade the drawn line as future work.

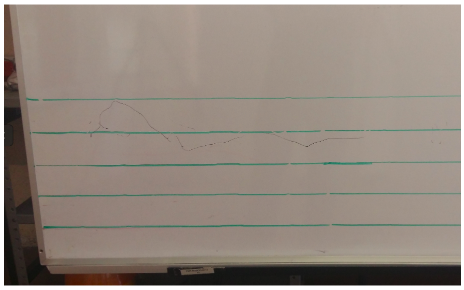

Figure 11: Line drawn by the drone.

6 CONCLUSIONS

This paper presents results regarding a control strategy to maintain a stable flight of the vehicle during the interaction task. The present work focuses on dealing with the stability problem of the arm, the wall-effect, and the contact with a surface. The strategy involves the use of GS- PID controller, where a set of operating points are carried out to create a group of controllers designed to eliminate the disturbances induced on the vehicle by the arm's motion. The conducted experiments prove that wall-effect degrades the efficiency of the GS-PID control, but the proper measure of these dynamic changes are considered in the control scheme to upgrade the performance of the system. The results indicate that the proposed approach is an improvement step towards the development of specific tasks of aerial manipulation systems. The main contribution of this work is the design of a GS-PID control technique for aerial interaction. The next step is to achieve a complete trajectory over the surface and replicate the results in outdoor scenarios. A video with the experiments and results is available the following link: https://youtu.be/mOFIo2YJJTE,

REFERENCES

[1] A. L. Luna, I. C. Vega, and J. M. Carranza. Gain-scheduling and pid control for an autonomous aerial vehicle with a robotic arm. In *2018 IEEE 2nd Colombian Conference on Robotics and Automation (CCRA)*, pages 1–6, Nov 2018.

[2] C. D. Bellicoso, L. R. Buonocore, V. Lippiello, and B. Siciliano. Design, modeling and control of a 5-dof light-weight robot arm for aerial manipulation. In *Control and Automation (MED), 2015 23th Mediterranean Conference on*, pages 853–858, June 2015.

[3] D. Bazylev, A. Kremlev, A. Margun, and K. Zimenko. Design of control system for a four-rotor uav equipped with robotic arm. In *Ultra Modern Telecommunications and Control Systems and Workshops (ICUMT), 2015 7th International Congress on*, pages 144–149, Oct 2015.

[4] T. Bartelds, A. Capra, S. Hamaza, S. Stramigioli, and M. Fumagalli. Compliant aerial manipulators: Toward a new generation of aerial robotic workers. *IEEE Robotics and Automation Letters*, 1(1):477–483, Jan 2016.

[5] Fabio Ruggiero, Jonathan Cacace, Hamid Sadeghian, and Vincenzo Lippiello. Passivity-based control of {VToL} {UAVs} with a momentum-based estimator of external wrench and unmodeled dynamics. *Robotics and Autonomous Systems*, 72:139 – 151, 2015.

[6] Basaran Bahadir Kocer, Tegoeh Tjahjowidodo, and Gerald Gim Lee Seet. Model predictive uav-tool interaction control enhanced by external forces. *Mechatronics*, 58:47 – 57, 2019.

[7] B. B. Kocer, G. S. G. Lee, and T. Tjahjowidodo. Nonlinear predictive uav-elastic tool interaction control in real-time. In *2018 IEEE/ASME International Conference on Advanced Intelligent Mechatronics (AIM)*, pages 472–477, July 2018.

[8] Lorenzo Marconi, Roberto Naldi, and Luca Gentili. Modelling and control of a flying robot interacting with the environment. *Automatica*, 47(12):2571 – 2583, 2011.

[9] S. Kannan, M. Alma, M. A. Olivares-Mendez, and H. Voos. Adaptive control of aerial manipulation vehicle. In *Control System, Computing and Engineering (ICCSCE), 2014 IEEE International Conference on*, pages 273–278, Nov 2014.

[10] S. Bouabdallah and R. Siegwart. Full control of a quadrotor. In *2007 IEEE/RSJ International Conference on Intelligent Robots and Systems*, pages 153–158, Oct 2007.

[11] F. Huber, K. Kondak, K. Krieger, D. Sommer, M. Schwarzbach, M. Laiacker, I. Kossyk, S. Parusel, S. Haddadin, and A. Albu-Schffer. First analysis and experiments in aerial manipulation using fully actuated redundant robot arm. In *2013 IEEE/RSJ International Conference on Intelligent Robots and Systems*, pages 3452–3457, Nov 2013.

[12] M. I. Sanchez, J. A. Acosta Acosta, and A. Ollero. Integral action in first-order closed-loop inverse kinematics. application to aerial manipulators. In *2015 IEEE International Conference on Robotics and Automation (ICRA)*, pages 5297–5302, May 2015.

[13] I. Palunko, A. Faust, P. Cruz, L. Tapia, and R. Fierro. A reinforcement learning approach towards autonomous suspended load manipulation using aerial robots. In *Robotics and Automation (ICRA), 2013 IEEE International Conference on*, pages 4896–4901, May 2013.

[14] Juhyeok Kim, Hai-Nguyen Nguyen, and Dongjun Lee. Preliminary control design on spherically-connected multiple-quadrotor manipulator system. In *Ubiquitous Robots and Ambient Intelligence (URAI), 2015 12th International Conference on*, pages 206–207, Oct 2015.

[15] Jing-Jing Xiong and En-Hui Zheng. Position and attitude tracking control for a quadrotor {UAV}. {*ISA*} *Transactions*, 53(3):725 – 731, 2014.

[16] I. Sadeghzadeh, A. Mehta, A. Chamseddine, and Y. Zhang. Active fault tolerant control of a quadrotor uav based on gainscheduled pid control. In *2012 25th IEEE Canadian Conference on Electrical and Computer Engineering (CCECE)*, pages 1–4, April 2012.

[17] Yeunduk Jung and David Hyunchul Shim. Development and application of controller for transition flight of tail-sitter uav. *J. Intell. Robotics Syst.*, 65(1-4):137–152, January 2012.

[18] Nour Ben Ammar, Soufiene Bouallgue, and Joseph Haggge. Fuzzy gains-scheduling of an integral sliding mode controller for a quadrotor unmanned aerial vehicle. *International Journal of Advanced Computer Science and Applications*, 9(3), 2018.